International Journal of Robotic Computing
Vol. 1, No. 2 (2019)

DOI: 10.35708/RC1868-126252

Simultaneous position and stiffness control of a revolute joint using a biphasic media variable stiffness actuator

Jesus H. Lugo*, Alessio Caligiuri, Matteo Zoppi, Giorgio Cannata, and Rezia Molfino

PMAR Laboratory, University of Genoa, Via all'Opera Pia, 15/a
Genoa, 16145,Italy
lugocalles@dimec.unige.it
www.pmar.robotics.unige.it

Received (11/02/2018)
Revised (06/11/2019)
Accepted (07/20/2019)

Abstract. Safe interactions between humans and robots are needed in several industrial processes and service tasks. Compliance design and control of mechanisms is a way to increase safety. This article presents a compliant revolute joint mechanism using a biphasic media variable stiffness actuator. The actuator has a member configured to transmit motion that is connected to a fluidic circuit, into which a biphasic control fluid circulates. Stiffness is controlled by changing pressure of control fluid into distribution lines. A mathematical model of the actuator is presented, a model-based control method is implemented to track the desired position and stiffness, and equations relating to the dynamics of the mechanism are provided. Results from force loaded and unloaded simulations and experiments with a physical prototype are discussed. This paper is an extended version of work presented in [1]. The additional information covers a detailed description of the system and its physical implementation.

Keywords: Biphasic media; variable stiffness actuator; stiffness control.

1 Introduction

Stiffness control in actuators is needed when a robot must perform motion tasks in the presence of humans, or when collisions with the environment are possible. For these scenarios, velocity and position should be sufficiently accurate while minimizing the risk of damaging humans, environment and itself [2]. Applications that require controllable stiffness can be identified as "robot-human

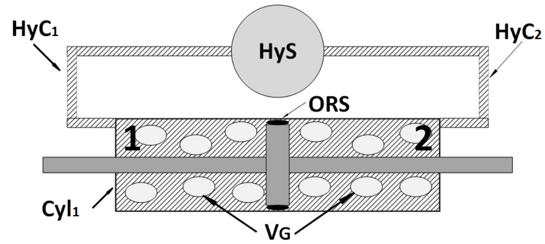

Fig. 1: Original embodiment of BMVSA. The compressible fraction is dispersed in the incompressible one

interaction" and "natural dynamics adjustment" [3]. The first one is focused on having a safer and more natural interaction between the human and the machine, while the second one deals with the adjustment of natural dynamics of the mechanical system in order to have a desired natural motion to reduce the energy consumption, legged robots for example [4].

Pneumatic actuators were implemented to achieve variable stiffness in robotic devices in [5]. This approach considers the dynamic characteristics of a pneumatic cylinder as a series elastic actuator, by replacing a four-way servo valve with a couple of three-way valves, which allows the user to modulate the stiffness and the output force. Model-based force and position controllers implemented in hydraulics circuits have been researched in [6]. The taken approach allowed the system to accurately propel a single DoF mechanism as an actuator of a Stewart platform.

Biphasic media variable stiffness actuators (BMVSA) have been extensively studied in [7,8,9,10,11,12,13,14]. These devices were designed using pneumatic and hydraulic components. A control fluid must be used in order to transmit motion into the circuit. This fluid is composed of two different non-mixable fluids, that can be liquid and/or gas. The gas works as nonlinear elastic element, altering the stiffness due to pressure variations, while the liquid is assumed incompressible and used to provide pressure changes and motion to the output link. Fig. 1 represents the primal embodiment of this approach, where confined gas fractions are dispersed in the liquid. As mentioned in [10], it is preferable that the gas is close to surface of the output link of the actuator, since the volume of liquid involved when an external force moves the output link and changes the pressures of the gas fractions is minimum. Some implementations of the system are industrial grippers for garment handling [11,12,13], surgical robotics concepts, suspension systems for mobile platforms [10] and actuation of revolute joints [9].

Based on the notations of Fig. 1, the actuator is composed of a double acting hydraulic cylinder *(Cyl1)* connected to a hydraulic circuit, inside which a control fluid circulates. The hydraulic circuit includes a supply and distribution system *(HyS)*. The circuit has two hydraulic distribution lines (*HyC1* and *HyC2*) respectively connected to the cylinder's chambers (1 and 2). The control fluid encompasses two different fluids in predefined proportions; in this case, liquid (mineral oil) and gas (N), having the compressible fluid dispersed in the chambers and considered as a total volume (*VG*). O-ring type seals *(ORS)* provide

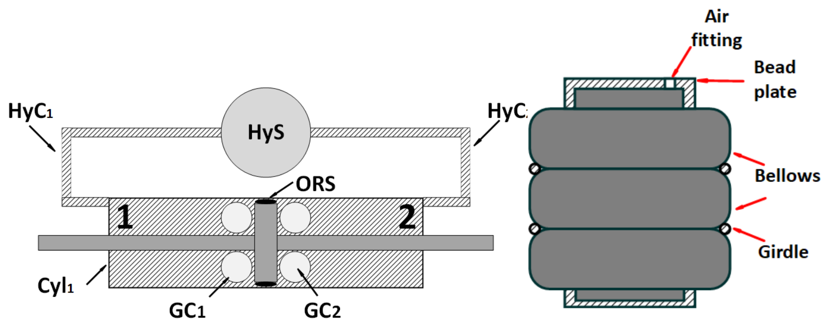

(a) Pneumatic containers BMVSA approach (b) Typical air spring
Fig. 2: BMVSA using pneumatic containers as compliant component

the translation of the piston without leakage. The hydraulic circuit must include elements that vary pressure inside the chambers with aim of controlling stiffness of the actuator, like pumps and valves.

BMVSA is considered to have antagonistic controlled stiffness, where two actuators with non-adaptable stiffness and nonlinear force-displacement characteristics are coupled antagonistically. Finally, it is assumed that the gas is considered ideal and the process is isothermal.

This document is an extended version of work presented in [1]. Information regarding modeling, control, and prototyping has been added to ease and improve the understanding of the system. The paper is organized as follows: Section 2 describes the possible architectures of this system, presents its mathematical model, and proposes a model-based controller for position and stiffness. Section 3 shows geometric and dynamic characteristics of the revolute joint. Section 4 discusses the results from simulations of the system. Section 5 analyses results from experiments done with the prototype. Section VI provides conclusions and ongoing work.

2 BMVSA architectures

The introduction of a compressible fluid into the system can be done in different ways, knowing that the fluids should not be miscible. Figure 2a displays an approach characterized by keeping the compressible fluid inside sealed elastic containers, shown as GC_1 and GC_2. These containers must be distributed inside the cylinder's chambers in a logical proportion, which adds a degree of complexity for the generation of the embodiment. One important feature is the relative fixed equilibrium position of the system when the circuit is open due to the fact that the containers occupy some part of the chambers' volumes. Pneumatic or air springs are devices that might serve for this purpose; they contain a column of air in an elastomeric bellow or sleeve, see Fig. 2b. They are commonly found in vehicle suspension systems, occasionally in conjunction with a coil spring, they are also used to insulate vibration in machinery and as linear or angular actuators [15].

Figure 3a is a design that shares the functioning principle of the hydro-pneumatic suspension (HPS) [16,17]. It is convenient due to its modularity, where

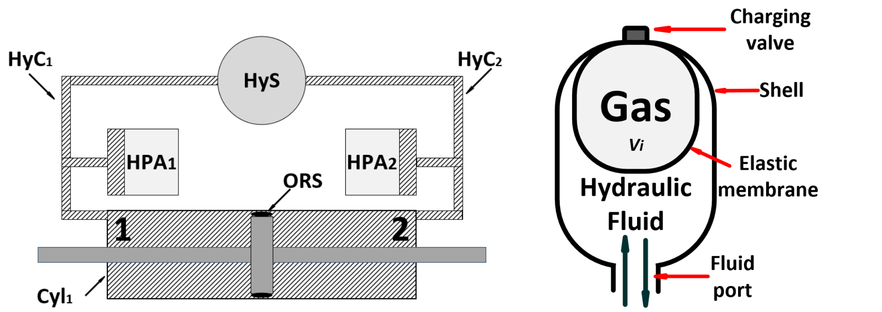

(a) HPA-BMVSA (b) Hydropneumatic accumulator schematic
Fig. 3: BMVSA using hydropneumatic accumulators as compliant component

the gas fraction is contained in hydro-pneumatic accumulators (HPA) that can be easily connected to the circuit and substituted if different gas characteristics are needed. The equilibrium position of the system is variable when the circuit is open because of HPA's volumes are not affecting the volume of the cylinder. The amount, size, distribution, type, and precharge of the HPA are design parameters that directly affects the stiffness of the system. Figure 3b displays a diaphragm type HPA defined by the use of a elastic diaphragm as separation membrane between the fluids.

2.1 Modeling of BMVSA

The following mathematical model is based on the HPA architecture, however, it can be applied for all the previously described configurations, with the only difference being the relation between the amount of incompressible fluid that can enter each chamber of the cylinder. The BMVSA is described as a damped harmonic oscillator in (1), where m is the mass of the output link of the actuator, (piston, seals and mechanical attachments), x_p is the displacement of the piston, k_v is the coefficient of viscosity, F_p is the force generated by the difference of pressures P_1 and P_2 acting on the piston's head surface S, as shown in (2), and F is an external force. From (1), it can be stated that F_p is taken as the restoring force of the system. The subscripts 1 and 2 denote chambers 1 and 2 and their corresponding HPAs.

$$m\ddot{x}_p + k_v\dot{x}_p - F_p = F \tag{1}$$

$$F_p = (P_1 - P_2)\, S \tag{2}$$

Considering an uniform temperature in the whole system, (3) can relate pressures and volumes.

$$P_i v_i = C_i \tag{3}$$

Where v_i is the volume of gas in the i^{th} HPA and C_i is the gas constant, which can be considered equal for both sides if the HPAs have the same characteristics ($C_i = C_1 = C_2$). In (4), the volumes are expressed as the sum of added oil volumes into the hydraulic circuit (v_{ai}) and the oil coming from the cylinder (Sx_p).

$$\begin{aligned} v_1 &= v_1(0) - v_{a1} - Sx_p \\ v_2 &= v_2(0) - v_{a2} + Sx_p \end{aligned} \tag{4}$$

The instantaneous stiffness K is the derivative of force generated by the difference of pressures in the cylinder with respect to displacement. Equation (5) shows that stiffness is a function of v_{ai}. If fluid is added to both chambers, the volumes of gas reduce and the pressures increase. Similarly, if fluid is subtracted from both chambers, the volume of gas increases and the pressure in both chambers reduces.

$$K = \frac{\partial F_p}{\partial x_p} = CS^2 \left(\frac{1}{v_1^2} + \frac{1}{v_2^2} \right) \tag{5}$$

2.2 Design considerations

In order to design an actuator that uses hydraulic and pneumatic components, the following design considerations must be accounted [17].

- Optimal selection of sealing elements, seal geometry and the seal material, must be performed in the beginning of the system layout. In particular the seal diameters have a great influence: the larger the seal diameter, the longer the length of the sealing edges and the higher the friction forces.
- Precharge of compressible fluid. Correct precharge involves accurately filling an accumulator's gas side with a dry inert gas, while no hydraulic fluid is in the fluid side. The precharge pressure selected will set the minimum stiffness that the system can provide.
- Dimensioning of components. Depending on the pressure, the elements must have dimensions that can provide the right amount of active area and enough mechanical stability to withstand inner pressure loads. It is essential to consider that dynamic pressure variations add to the pressure in static state(design position).
- Dimensioning and type of hydraulic cylinder. The piston diameter is determined by making the maximum use of the available system pressure. Rod diameter and cylinder stroke are defining parameters for a cylinder which are completely dependent on the type of external system's load and task.
- Selection and positioning of hydraulic lines and fittings. The circuit lines are important since the hydraulic fluid in the lines is in permanent motion and their flow restriction effect has a direct influence on the system's behavior. Due to the high flow rates, the diameter of these lines should be chosen to be as large as possible.

2.3 Model-based controller

It is possible to design a control strategy able to manipulate the position and the stiffness of the system simultaneously. The usual method to control position in a hydraulic cylinder is performed by controlling the pressures in both chambers, hence, movement is done whenever the pressures are different. The approach for the stiffness is similar but it is related to the amount of pressure in each chamber: the higher the pressure, the higher the stiffness, and vice versa. Model-based tracking for nonlinear systems is a part of control where tracking is goal and a controller is based upon a dynamic model [20]. Model-based control outperforms kinematic-based control with regard to performance, control precision, ability to cope with external disturbances, friction, and noise.

The functional characteristics of the actuator depend on its design and the initial conditions. The measured quantities in the system are: *(i)* the position of the piston, and *(ii)* the pressures in the chambers. Equations (6) describe the volumetric flow rate, where q_i represents the moving volume in the system's chambers ($\dot{v_{ai}} = q_i$). At any instant, the volume subtracted or added fluid cannot be larger than the total volume of gas since the liquid fraction is considered incompressible.

$$\begin{aligned} \dot{v_1} &= -q_1 - S\dot{x_p} \\ \dot{v_2} &= -q_2 + S\dot{x_p} \end{aligned} \tag{6}$$

Equation (7) was deduced considering u as spring's restoring force equal to F_p and x_p^* as the desired position, where K_E is the characteristic gain of the spring and u^* is the desired control signal. The error of position is stated in (8) and its derivative with respect to time in (9), where γ is the tuning parameter to achieve minimal error.

$$u^* = -K_E(x_p - x_p^*) \tag{7}$$

$$e = u - u^* \tag{8}$$

$$\dot{e} = \dot{F_p} - \dot{u^*} = -\gamma e \tag{9}$$

From the combination of (2) and (9) it is possible to write:

$$\dot{e} = \frac{S}{C}\left[{P_2}^2\dot{v_2} - {P_1}^2\dot{v_1}\right] - \dot{u^*} \tag{10}$$

Substituting (6) into (10) leads to:

$$\dot{e} = \frac{S}{C}\left[{P_1}^2 q_1 - {P_2}^2 q_2\right] - w_{xp}(t) \tag{11}$$

$$w_{xp}(t) = -\frac{S^2\dot{x_p}}{C}\left({P_1}^2 + {P_2}^2\right) + \dot{u}^* \tag{12}$$

From substituting (9) into (11), the equation that controls the position of the system is obtained (13).

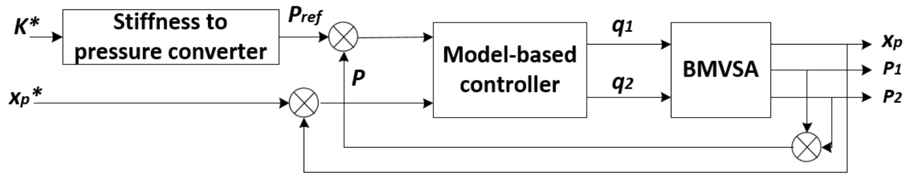

Fig. 4: Model-based controller schematic

$$
\begin{aligned}
b_{xp}(t) &= {P_1}^2 q_1 - {P_2}^2 q_2 \\
b_{xp}(t) &= \frac{C}{S}\left(-\gamma e + w_{xp}(t)\right)
\end{aligned}
\tag{13}
$$

Based on equation (5), it is possible to confirm that the direct relation between pressures and stiffness of the systems allows controlling the stiffness of the system. The pressure control equations were developed following the previous procedure used for position control. The error of pressure is used to control the stiffness, which is defined as the difference between the current pressures of the system and the ones related to desired stiffness (P_{ref}), as shown in (14).

$$e_p = \left(\frac{P_1 + P_2}{2} - P_{\mathrm{ref}}\right) \tag{14}$$

Differentiating (14) with respect to time and substituting (6) leads to:

$$\dot{e_p} = \left(\frac{1}{2C}\right)\left((P_1)^2 q_1 + (P_2)^2 q_2\right) + w_p(t) \tag{15}$$

$$w_p(t) = \frac{S^2 \dot{x_p}}{2C}\left({P_1}^2 + {P_2}^2\right) - \dot{P}_{\mathrm{ref}} \tag{16}$$

$\dot{e_p}$ is described in (17), where λ is the tuning parameter to achieve minimal error.

$$\dot{e_p} = -\lambda e_p \tag{17}$$

After substituting (15) into (17), the equation (18) is used to control the pressure.

$$b_p(t) = -2C\left(\lambda e_p + w_p(t)\right) \tag{18}$$

Expanding and solving (9) and (17) for q_i allows to control the position and stiffness of the system as shown in (19), (20), (13), (18), (12) and (16).

$$\begin{bmatrix} q_1 \\ q_2 \end{bmatrix} = \begin{bmatrix} {P_1}^2 \\ -{P_2}^2 \end{bmatrix} D b_{xp}(t) + \begin{bmatrix} {P_1}^2 \\ {P_2}^2 \end{bmatrix} D b_p(t) \tag{19}$$

$$D = \frac{1}{{P_1}^4 + {P_2}^4} \tag{20}$$

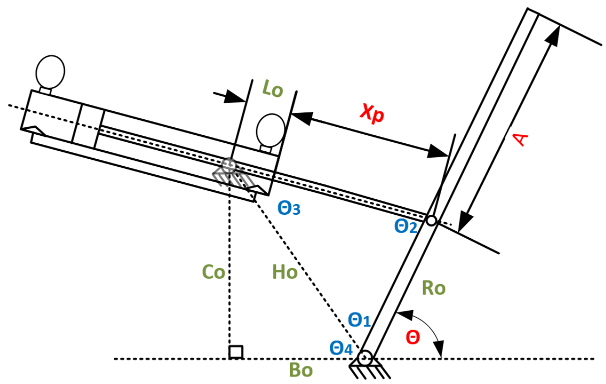

Fig. 5: Diagram of revolute joint mechanism

Based on the previous equations, an array of hydraulic proportional flow valves can be used to the vary the pressures in both chambers. The schematic that represents the aforementioned controller is shown in Fig. 4.

3 Revolute joint

A revolute joint mechanism has been designed to visualize the effect of the stiffness variation of the actuator, as shown Fig. 5. This mechanism has one DoF and its geometric parameters are given in Table 1. Equations (21) and (22) relate linear displacement (xp) with angular displacement (θ).

$$cos(\theta_1) = \frac{C_o}{H_o} sin(\theta) + \frac{B_o}{H_o} cos(\theta) \tag{21}$$

$$x_p + L_o = \left(R_o^2 + H_o^2 - 2R_oH_ocos(\theta_1)\right)^{\frac{1}{2}} \tag{22}$$

3.1 Stiffness analysis

The output link works as a rotational actuator. Its torque, called τ_{joint}, is produced by F_p. Equations (23), (24), and (25) provide its definition.

Table 1: Geometric parameters

Parameter	Length (m)
L_o	0.07
C_o	0.1
B_o	0.105
H_o	0.145
R_o	0.12
A	0.245
$x_p$max	0.15
$x_p$min	0

$$\tau_{\text{joint}} = (SCR_o)\left(\frac{1}{v_1} - \frac{1}{v_2}\right) sin(\theta_2) \tag{23}$$

$$sin(\theta_2) = \frac{H_o}{x_p + L_o}\left(\frac{B_o}{H_o} sin(\theta) + \frac{C_o}{H_o} cos(\theta)\right) \tag{24}$$

$$\tau_{\text{joint}} = \tau_w + \tau_I + \tau_{F_{ext}} \tag{25}$$

τ_w is the torque generated by the weight of the equivalent mass, given by $m_{eq} = m_{\text{Load}} + m_{\text{Link}}$, at the center of mass ($R_{m_{eq}}$) on the output link, as shown in (26) and (27).

$$\tau_w = m_{eq} g R_{m_{eq}} sin\left(\frac{\pi}{2} - \theta\right) \tag{26}$$

$$R_{m_{eq}} = \left[m_{\text{Load}}\left(R_o + \frac{A_o}{2}\right) + m_{\text{Link}}\left(\frac{R_o}{2}\right)\right]\frac{1}{m_{eq}} \tag{27}$$

τ_I is the torque caused due to the inertia of the equivalent mass, as defined in (28). An external force has been considered to be applied at the end of the output link, producing $\tau_{F_{\text{ext}}}$, as shown in (29).

$$\tau_I = \frac{m_{eq} g (R_{m_{eq}})^2 \ddot{\theta}}{3} \tag{28}$$

$$\tau_{F_{\text{ext}}} = F_{\text{ext}}\left(R_o + A_o\right) \tag{29}$$

The instantaneous rotational stiffness $K(\theta)$ of the mechanism is the derivative of τ_{joint} with respect to the θ, as defined in (30).

$$K(\theta) = \frac{\partial \tau_{\text{joint}}}{\partial \theta} \tag{30}$$

The previous equations demonstrate that $K(\theta)$ is a function of the output force (F_p) and the angular displacement (θ), and it is affected by the weight of the equivalent mass.

4 Simulation

The following simulation was performed to study the stiffness and position of the model using the parameters given in Table 2. Two types of tests were performed: the first did not have an external force applied, while the second one had a force signal with a square wave shape with 10 N amplitude and baseline on 0 N at 0.2 Hz. Both types of simulations were executed including the m_{Load} and m_{Link}. Position in the actuator is measured from left end of the cylinder to its right end.

The desired position is given as a sinusoidal signal with 0.23 radians amplitude and baseline on 1.23 radians at 0.05 Hz (to approximate a linear displacement in the cylinder with amplitude of 0.025 m and a baseline on 0.075 m), as

Table 2: Simulation parameters for mechanism

Parameter	**Value**
m	$1\ Kg$
m_{Load}	$3.8\ Kg$
m_{Link}	$1\ Kg$
K_v	$0.5\ Ns/m$
K_E	$3x10^3\ N/m$
S	$3.776x10^{-4}\ m^2$
C	$300\ Pam^3$
γ	$-5x10^2$
λ	$-1.3x10^3$
$x_p(0)$	$0.075\ m$
$v_i(0)$	$1.5x10^{-4}\ m^3$

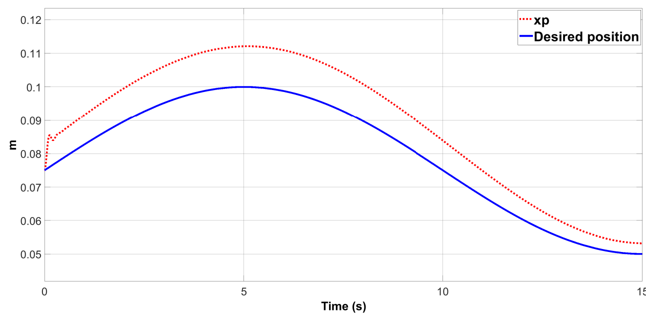

Fig. 6: Position tracking in BMVSA without external force

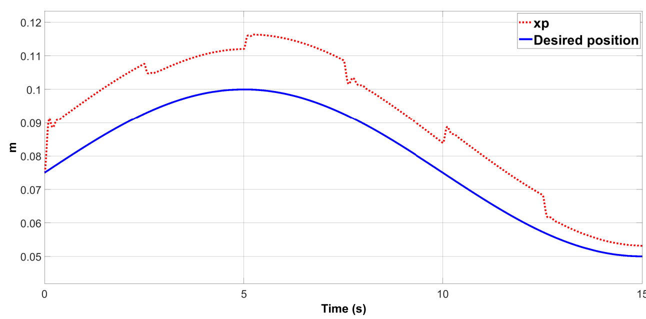

Fig. 7: Position tracking in BMVSA with external force

shown in Figs. 6, 7, 8, and 9, while the desired stiffness is a sinusoidal signal with 20 Nm/radians amplitude and baseline on 80 Nm/radians at 0.1 Hz, as depicted in Fig. 10.

The results of the simulations prove that the model-based controller is able to properly track position and stiffness even if the desired signals to follow are nonlinear, as illustrated in Figs. 8 and 10. It is worth to note that the controller was tuned to prioritize stiffness tracking over position tracking as displayed in Fig. 7 and 9, where the desired position in never reached, while the desired mechanism stiffness is always obtained, see Fig. 11, 13 and 15. It can be stated

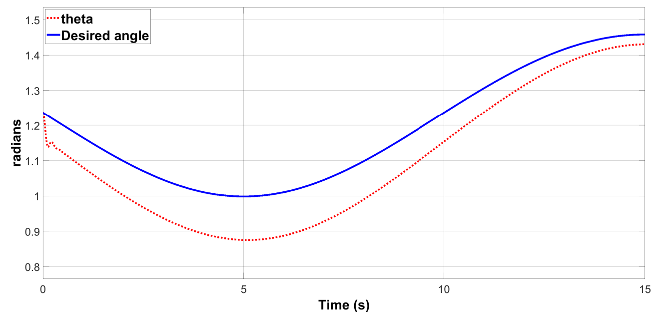

Fig. 8: Angle tracking in mechanism without external force

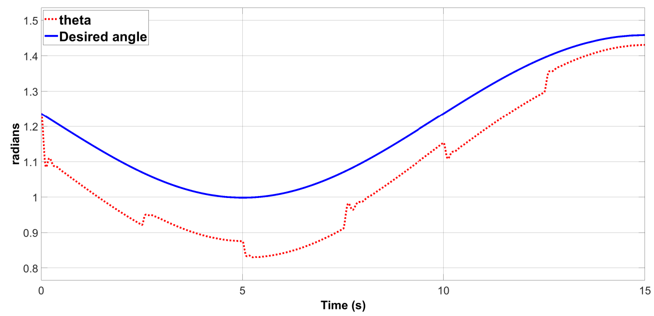

Fig. 9: Angle tracking in mechanism with external force

Fig. 10: Stiffness tracking in mechanism without external force

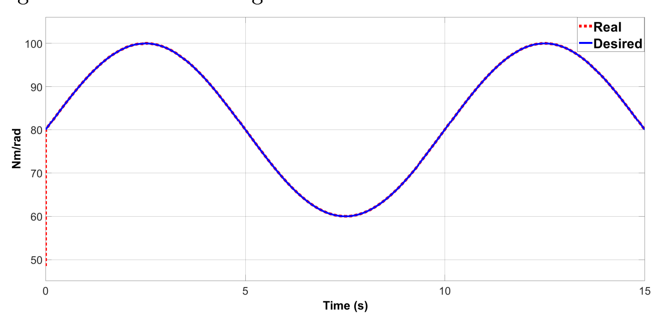

Fig. 11: Stiffness tracking in mechanism with external force

that whenever a load force differs from zero a displacement in the actuator is generated, which is directly related to the value of K_E.

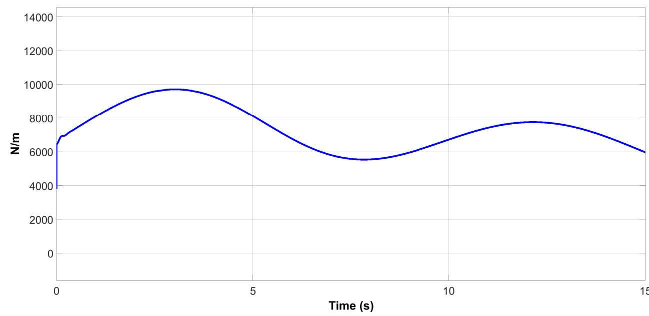

Fig. 12: Stiffness tracking in BMVSA without external force

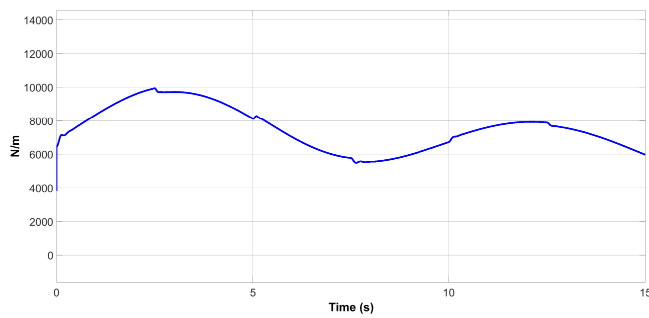

Fig. 13: Stiffness tracking in BMVSA with external force

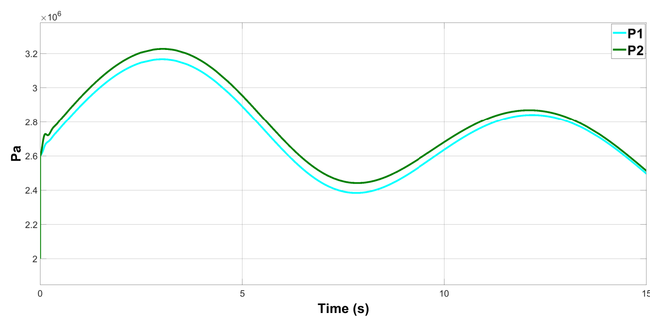

Fig. 14: Pressures in BMVSA without external force

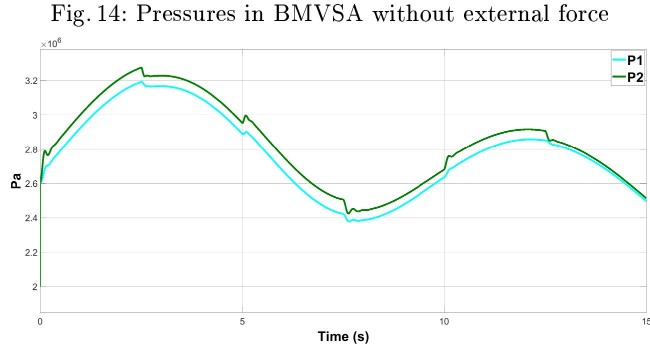

Fig. 15: Pressures in BMVSA with external force

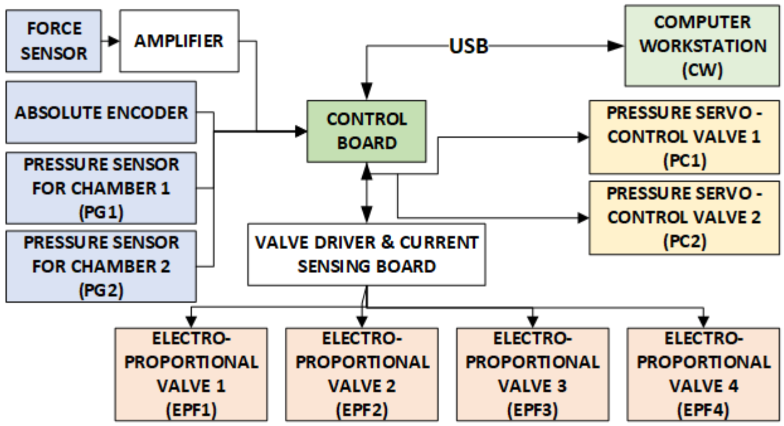

Fig. 16: Experimental setup electronic control diagram

5 Prototype setup

The BMVSA and the mechanism have been prototyped and tested. The mechanism is made of steel and it keeps geometry and sizes mentioned in Table 1. It is worthy to mention that most of the components are off-the-shelf, even the custom made control and valve driver boards can be replaced by industrial level control systems. The compression ratio (Co_R) is a physical characteristic of HPA that relates the maximum pressure that the accumulator can hold to its initial pressure before its rubber diaphragm wears out considerably. Figure 17 shows a schematic of the implemented hydraulic circuit. Its main components are the hydraulic cylinder (*Cyl1*), a pair of HPAs (*AC1-2*), a hydraulic pump (*HyS*), two pressure gauges (*PG1-2*), four electro-proportional flow control valves (*EPF1-4*) and two proportional pressure control valves (*PC1-2*). The purpose of having two pressure control valves is to isolate the hydraulic input for each chamber of the cylinder. The maximum flow, the maximum working pressure, the maximum difference of pressures between input and output and PWM frequency (10 liters/second, 350 bar, 15 bar, and 120 Hz, respectively for the selected valves) are *EPF*'s performance characteristics that limit the actuator to work within their physical limits, Fig. 18a displays the designed array of EPF valves and Fig.18b shows the pump and the PC valves. Fig. 19 shows the prototype in unloaded state.

The previously described model-based controller provides a solution for q_1 and q_2; to obtain the desired flows, a set of four *EPF* is used, two per chamber, see 18a. The position of the piston is measured via encoder and the stiffness is calculated in real-time using the pressure gauges. The tuning parameters and initial conditions are given in Table 3. It is worth to mention that a pin shaped force gauge (*FG*) is used as the rotation pin that connects the cylinder and the arm. *FG* will be used for measuring the output force of the actuator in future experiments.

A custom-designed control board powered by a multi-threaded ARM microprocessor is used to run the controller on real-time. It was designed by SWHARD

S.R.L. and was intended for a prototyping use [18]. This board contains drivers for valves running at 120 Hz for each of *EPF* and uses serial communication with the CW. The valve driver and current sensing board contains EPF valves current drivers and works with a maximum frequency of 8 Hz. Figure 16 displays the electronic control diagram of the system, where, the main control component is the computer workstation (CW). The control board is used as an interface between the CW, sensors and valves. The valves driver and current sensing board, which its main function is provide coil's current measurements from each individual *EPF* valve in order to read its relative state to the control board, and control the flow of the same devices [18].

6 Experiments with the prototype

Only loaded experiments were performed. A 3.8 kg metal bar is used to load the output link. Due to prototype's physical features, the desired position is given as a sinusoidal signal with 0.5 radians amplitude and baseline on 1.2 radians at 0.05 Hz, while the desired stiffness is a sinusoidal signal with 20 Nm/radians amplitude and baseline on 80 Nm/radians at 0.1 Hz.

The results of the experiments confirm that the model-based controller can track position and stiffness, as depicted in Figs. 20, 21, 22 and 23. Like in the simulations, the controller prioritized stiffness tracking over position tracking.

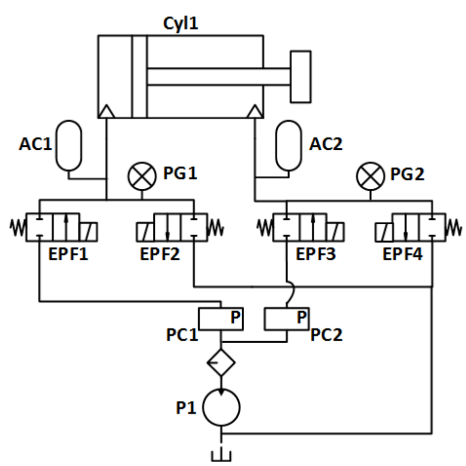

Fig. 17: Hydraulic system schematic

Table 3: Experiment parameters

Parameter	Value
K_v	$0.5\ Ns/m$
K_E	$2x10^4\ N/m$
γ	$-6.5x10^3$
λ	$-2.5x10^3$
$x_p(0)$	$0.075\ m$
Co_R	4

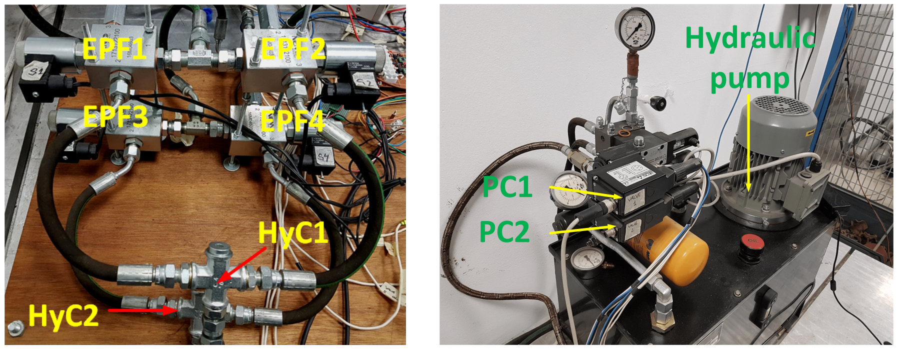

(a) Electro-proportional valves array. (b) Hydraulic pump setup.

Fig. 18: BMVSA hydraulic components. A couple of pressure control valves are connected to the output of the pump to control the pressure that is provided to the system.

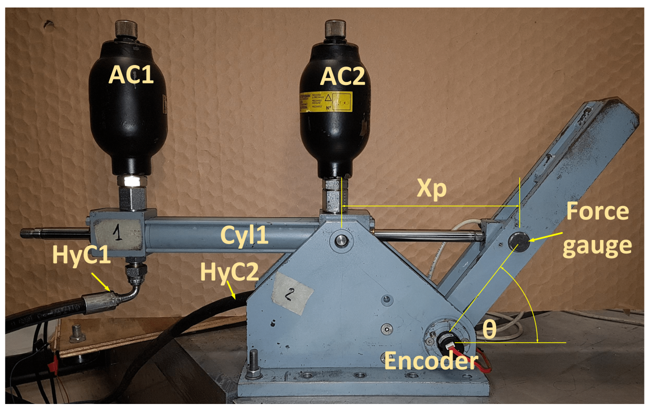

Fig. 19: Prototype of mechanism

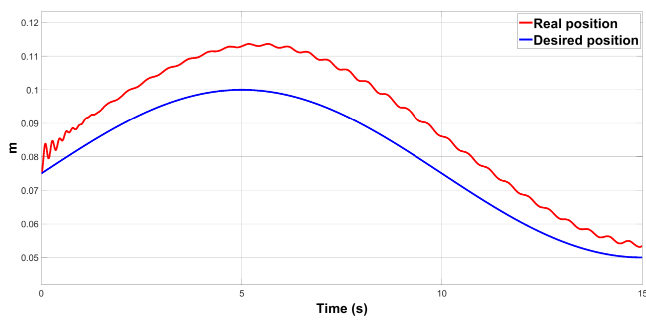

Fig. 20: Position tracking during experiment

Another presented phenomena that appear during the experiments are small jumps in the position, as shown 20 and 21, these are related to the static friction of the piston, the friction in mechanism joints, and the low frequency in which the *EPF*s work.

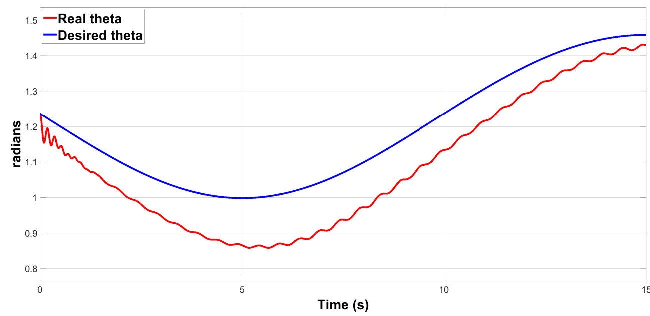

Fig. 21: Angle tracking during experiment

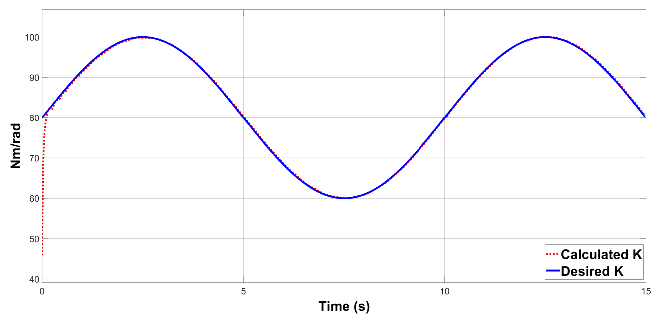

Fig. 22: Estimated rotational stiffness tracking during experiment

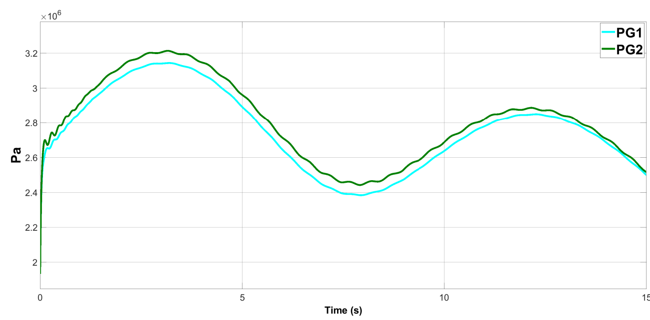

Fig. 23: Measurements of pressure gauges

7 Conclusion

The stiffness of the BMVSA is related to the pressures of the gas fractions contained in the accumulators. This device has two advantages due to its biphasic nature: the hydraulic system gives it the possibility to have a high output force, while the nonlinearity of the gas provides a wider range of stiffness than the VSAs using traditional elastic components.

The results obtained from simulations demonstrate that the model-based controller approach can accurately track desired stiffness and approximate the desired position, while an external force acts on it. The measurements taken during the experiments corroborate the previously mentioned about the simulations, pointing out the influence of the output link's mass, friction and load's inertia.

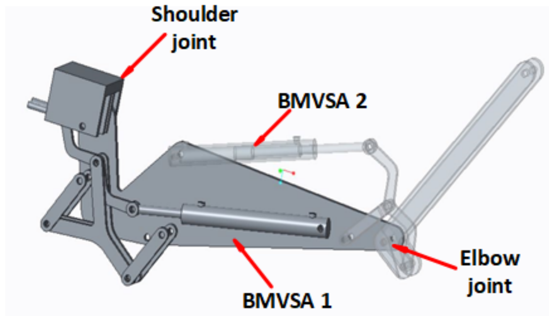

Fig. 24: CAD model of 2 DoF anthropomorphic arm driven by 2 VSAs

Modeling and design of rehabilitation devices, prosthesis, and orthoses are a well known applications for VSAs. Nowadays, the technology developed in this project is being used for designing these devices. In [19], a 2 DoF anthropomorphic arm has been designed using BMVSAs to drive them, see Fig 24. This prosthesis is characterized by the use of Hoeken linkages to keep a constant velocity during the movements.

Momentum-based collision detection methods [21] and reaction algorithms are being tested in the system to increase the safety during physical interaction. The monitoring of collisions is done using residuals of the momentum of the mechanism without knowledge of the joint torque or stiffness. The reaction algorithms allow the robot to stop its motion and to reduce its stiffness for the sake of safety of its structure and the colliding object.

References

1. J. H. Lugo, A. Caligiuri, M. Zoppi, G. Cannata and R. Molfino, *"Position and Stiffness Control of One DoF Revolute Joint Using a Biphasic Media Variable Stiffness Actuator,"* in 2019 Third IEEE International Conference on Robotic Computing (IRC), pp. 308-314, 2019.
2. B. Vanderborght, A. Albu-Schaffer, A. Bicchi, E. Burdet, D. G. Caldwell, R. Carloni, M. Catalano, O. Eiberger,W. Friedl, G. Ganesh, et al. *"Variable impedance actuators: A review,"* Robotics and autonomous systems, vol. 61 (12), pp. 1601–1614, 2013.
3. R. Van Ham, T. G. Sugar, B. Vanderborght, K. W. Hollander, and D. Lefeber, *"Compliant actuator designs"*, IEEE Robotics and Automation Magazine, vol. 16 (3), 2009.
4. C. Semini, N. Tsagarakis, E. Guglielmino, F. Cannella, and D.G. Caldwell, *"Design of HyQ – a hydraulically and electrically actuated quadruped robot,"* Proceedings of the Institution of Mechanical Engineers, Part I: Journal of Systems and Control Engineering, vol 225 (6), 2011.
5. X. Shen, and M. Goldfarb, *"Simultaneous Force and Stiffness Control of a Pneumatic Actuator"*, Journal of Dynamic Systems, Measurement, and control, vol. 129, pp. 425-434, 2007.
6. I. Davliakos, and E. Papadopoulos, *"Development of a Model-Based Nested Controller for Electrohydraulic Servos,"* Proceedings of the 2005 IEEE International Symposium on, Mediterrean Conference on Control and Automation Intelligent Control, pp. 107-112, 2005.

7. M. Zoppi, "Method for adapting stiffness in a variable stiffness actuator," US Patent 8 991 169, March 31, 2015.
8. B. Han, M. Zoppi, and R. Molfino, *"Variable impedance actuation using biphasic media,"* Mechanism and Machine Theory, vol. 62, pp. 1-12 , 2013.
9. B. Han, M. Zoppi, and R. Molfino, *"Variable impedance actuation meso-micro physical models and rotation link using biphasic media,"* Procedia Engineering, vol. 64, pp. 1020–1029 , 2013.
10. B. Han, *"Variable impedance actuation using biphasic media,"* Ph.D. Thesis dissertation, University of Genoa, 2013.
11. L. Le, M. Zoppi, M. Jilich, R. Camoriano, D. Zlatanov, and R. Molfino, *"Development and analysis of a new specialized gripper mechanism for garment handling,"* in ASME 2013 International Design Engineering Technical Conferences and Computers and Information in Engineering Conference, pp. V06BT07A013–V05BT08A023, 2013.
12. L. Le, M. Zoppi, M. Jilich, B. Han, D. Zlatanov, and R. Molfino, *"Application of a biphasic actuator in the design of a robot gripper for garment handling,"* in ASME 2014 International Design Engineering Technical Conferences and Computers and Information in Engineering Conference, pp. V05BT08A022–V05BT08A022, 2014.
13. L. Le, M. Zoppi, M. Jilich, B. Han, D. Zlatanov, and R. Molfino, *"Application of a biphasic actuator in the design of the clopema robot gripper,"* Journal of Mechanisms and Robotics, vol. 7, pp. 011011(1-8), 2015.
14. J.H. Lugo, G. Cannata, M. Zoppi, and R. Molfino, *"Modeling and Simulation of a Biphasic Media Variable Stiffness Actuator,"* International Journal of Mechanical Engineering and Robotics Research, 2018.
15. J. H. Lugo, *"Design, modeling and implementation of a biphasic media variable stiffness actuator,"* Ph.D. Thesis dissertation, University of Genoa, 2019.
16. W. Bauer, H. Schwegler , *"Hydro-pneumatic suspension system,"* US Patent 7 219 779, May 22, 2007.
17. W. Bauer, *"Hydropneumatic suspension systems,"* Springer Science and Business Media, 2010.
18. A. Caligiuri, *"Position and stiffness control of one DoF revolute joint using a biphasic media variable stiffness actuator,"* Master Thesis dissertation, University of Genoa, 2018.
19. O. Hryshaienko , *"Designing of a biphasic variable stiffness actuator for driving the 2-DOF anthropomorphic arm,"* Master Thesis dissertation, Warsaw University of Technology, 2019.
20. E. Jarzebowska„ *"Model-based tracking control of nonlinear systems,"* Chapman and Hall/CRC, 25, 2016.
21. F. Flacco, A. De Luca, I. Sardellitti, and N. Tsagarakis, *"On-line estimation of variable stiffness in flexible robot joints,"* The International Journal of Robotics Research, vol 31 (13), pp. 1556–1577, 2012.